Simulation of shock wave boundary layer interaction in flat channel with jet injection

Nurtoleu Shakhan, Asel Beketaeva, and Altynshash Naimanova

Citation: AIP Conference Proceedings **1759**, 020102 (2016); doi: 10.1063/1.4959716
View online: http://dx.doi.org/10.1063/1.4959716
View Table of Contents: http://scitation.aip.org/content/aip/proceeding/aipcp/1759?ver=pdfcov
Published by the AIP Publishing

Simulation of shock wave boundary layer interaction in flat channel with jet injection

Nurtoleu Shakhan*, Asel Beketaeva† and Altynshash Naimanova†

*Al-Farabi Kazakh National University, Almaty, Kazakhstan
†Institute of Mathematics and Mathematical Modeling, Almaty, Kazakhstan

Abstract. A multispecies supersonic gas flow in the flat channel with perpendicular jet injection is numerically simulated by using the Favre-averaged Navier-Stokes equations coupled with $k-\omega$ turbulence model. High order WENO scheme is applied to approximate convective terms. During the investigation of flow physics in detail, the three shock-wave structures are observed: in the region of the jet (barrel, bow, oblique and closing shocks), on the upper boundary layer (reflection, transmitted and reattachment shocks), and new structures behind the jet on the lower boundary layer, which are analogous to the structures on the upper boundary layer.

Keywords: Supersonic flow, SWBLI, Flow control, Separation, Navier-Stokes equations, WENO scheme, Shock wave
PACS: 02.60.Cb, 02.70.Bf

INTRODUCTION

The flow around jets has been comprehensively investigated experimentally [1, 2] and numerically simulated. Nowadays the interactions between boundary layer and shock wave in the channel flow field with perpendicular jet injection aren't well understood. Due to complexity of these interactions, usually they are studied by parts. One part of these studies focuses on the properties of shock-wave structures in the region of the jet injection [3, 4], other considers the zone of shock wave boundary layer interaction [5, 6]. In the present paper, we simulate and study the shock-wave structures in the supersonic channel flow with jet injection where both processes will be present.

THE FORMULATION OF THE PROBLEM

Supersonic flow of air with transverse jet injection from the bottom wall of rectangular channel is considered. The system of two-dimensional Favre averaged Navier-Stokes equations for multicomponent gaseous mixture in Cartesian coordinate system in conservative form is presented as

$$\frac{\partial \vec{U}}{\partial t}+\frac{\partial\left(\vec{E}-\vec{E}_v\right)}{\partial x}+\frac{\partial\left(\vec{F}-\vec{F}_v\right)}{\partial z}=0, \tag{1}$$

$$\vec{U}=\left(\rho,\rho u,\rho w,E_t,\rho Y_k,\rho k,\rho\omega\right)^T,$$

$$\vec{E}=\left(\rho u,\rho u^2+P,\rho uw,\left(E_t+P\right)u,\rho uY_k,\rho uk,\rho u\omega\right)^T,$$

$$\vec{F}=\left(\rho w,\rho uw,\rho w^2+P,\left(E_t+P\right)w,\rho wY_k,\rho wk,\rho w\omega\right)^T,$$

$$\vec{E}_v=\left(0,\tau_{xx},\tau_{xz},u\tau_{xx}+w\tau_{xz}-q_x,J_{xk},\frac{1}{Re}(\mu_l+\sigma_k\mu_t)\frac{\partial k}{\partial x},\frac{1}{Re}(\mu_l+\sigma_\omega\mu)\frac{\partial\omega}{\partial x}\right)^T,$$

$$\vec{F}_v=\left(0,\tau_{xz},\tau_{zz},u\tau_{xz}+w\tau_{zz}-q_z,J_{zk},\frac{1}{Re}(\mu_l+\sigma_k\mu_t)\frac{\partial k}{\partial z},\frac{1}{Re}(\mu_l+\sigma_\omega\mu)\frac{\partial\omega}{\partial z}\right)^T,$$

International Conference on Analysis and Applied Mathematics (ICAAM 2016)
AIP Conf. Proc. 1759, 020102-1–020102-5; doi: 10.1063/1.4959716
Published by AIP Publishing. 978-0-7354-1417-4/$30.00

$$P = \frac{\rho T}{\gamma_\infty M_\infty^2 W}, \quad W = \left(\sum_{k=1}^{N_p} \frac{Y_k}{W_k} \right)^{-1}, \quad \sum_{k=1}^{N_p} Y_k = 1,$$

$$E_t = \frac{\rho}{\gamma_\infty M_\infty^2} h - P + \frac{1}{2}\rho \left(u^2 + w^2 \right), \quad h = \sum_{k=1}^{N_p} Y_k h_k, \quad h_k = h_k^0 + \int_{T_0}^{T} c_{pk} dT,$$

$$c_{pk} = C_{pk}/W_k, \quad \tau_{xx} = \frac{\mu}{Re}\left(2u_x - \frac{2}{3}\left(u_x + w_z \right) \right),$$

$$\tau_{xx} = \frac{\mu}{Re}\left(2w_z - \frac{2}{3}\left(u_x + w_z \right) \right), \quad \tau_{xz} = \tau_{zx} = \frac{\mu}{Re}\left(u_z + w_x \right),$$

$$q_x = \left(\frac{\mu}{PrRe} \right) \frac{\partial T}{\partial x} + \frac{1}{\gamma_\infty M_\infty^2} \sum_{k=1}^{N_p} h_k J_{xk}, \quad q_z = \left(\frac{\mu}{PrRe} \right) \frac{\partial T}{\partial z} + \frac{1}{\gamma_\infty M_\infty^2} \sum_{k=1}^{N_p} h_k J_{zk},$$

$$J_{xk} = -\frac{\mu}{ScRe} \frac{\partial Y_k}{\partial x}, \quad J_{zk} = -\frac{\mu}{ScRe} \frac{\partial Y_k}{\partial z}.$$

The system of equations (1) is written in dimensionless form using conventional notations, the flow parameters $(u_\infty, \rho_\infty, T_\infty, W_\infty)$, are taken as reference values, the pressure P and the total energy E_t are related to the value $\rho_\infty u_\infty^2$, the specific enthalpy h_k to $R^0 T_\infty / W_\infty$, the molar specific heats C_{pk} to R^0, and the slot width is chosen as the reference length scale. Value Y_k is mass concentration of component, index of mass concentration $k = 1$ corresponds to O_2, $k = 2$ is for H_2 (or He) and $k = 3$ is for N_2, $N_p = 3$ is the amount of the components in gaseous mixture. W_k is molecular weight of component, Re, Pr, and Sc are Reynolds, Prandtl and Schmidt numbers respectively, $\tau_{xx}, \tau_{zz}, \tau_{xz}, \tau_{zx}$ are viscous stress tensors, q_x, q_z, J_{xk}, J_{zk} are heat and diffusive fluxes (diffusive fluxes are computing by the Fick's law), $\mu = \mu_l + \mu_t$ is coefficient of dynamic viscosity which is summation of laminar and turbulent viscosities. For determining μ_t, two-parametric $k - \omega$ turbulence model is used.

THE INITIAL AND BOUNDARY CONDITIONS

On the entrance, the parameters of flow are set as

$$Y_k = Y_{k\infty}, W_k = W_{k\infty}, P = P_\infty, T = T_\infty,$$

$$u = M_\infty \sqrt{\gamma_\infty R_0 T_\infty / W_\infty}, w = 0, \qquad x = 0, \quad 0 \le z \le H.$$

The boundary layer is set to the inlet section near the wall, and the velocity approximated according to the power law as

$$u = 0,1 \left(\frac{z}{\delta_2} \right) + 0,9 \left(\frac{z}{\delta_2} \right)^2, \qquad x = 0, \quad 0 \le z \le \delta_2,$$

where $\delta_2 = 0.2\delta_1$ is thickness of the viscous-buffer sublayer (20% from the thickness of the boundary layer), $\delta_1 = 0.37x(Re)^{-0.2}$ is thickness of the boundary layer. The viscous-buffer sublayer is in the range of $z^+ \le 70$, where $z^+ = \delta_2(u_\tau Re_x)$ is distance from the wall, non-dimensionalised by the viscous length scale, $u_\tau = (0.5C_f)^{0.5} u_\infty$ is dynamic velocity, C_f is skin friction coefficient.

The degree law is considering for fully turbulent boundary layer. The thickness of this boundary layer is determined by $z^+ \geq 70$.

On the bottom and top wall:

$$u = w = 0, \frac{\partial T}{\partial z} = \frac{\partial P}{\partial z} = \frac{\partial Y_k}{\partial z} = 0, \qquad z = 0, H \quad 0 \leq x \leq L,$$

where L is length of plane and H is height of plane,

In the slot:

$$Y_k = Y_{k0}, W_k = W_{k0}, P = nP_\infty, T = T_0,$$

$$u = 0, w = M_0\sqrt{\gamma_0 R_0 T_0 / W_0}, \qquad z = 0, \quad L_b \leq x \leq L_b + h,$$

where L_b is distance from the entrance till the slot, D is width of slot, $n = P_0/P_\infty$ is pressure ratio, M_0 and M_∞ are the Mach numbers of jet and flow respectively, $0, \infty$ refers to the jet and flow parameters.

On the outlet, the non-reflecting boundary conditions are applying.

METHOD OF THE SOLUTION

For capturing the large gradients at the boundary layers of bottom and top walls, and at the slot level, the grid transformation procedure is applying. Parameters of the coordinate transformation are described in [7].

In the present study, first derivatives are approximated with the usage of WENO scheme, idea of which based on ENO scheme, presented in [8]. In WENO scheme during the interpolation of piece-constant polynomial function, the Newton polynomial of third order is applying and in spite of dealing with one candidate stencil, the convex combination of all candidate stencils with weighted coefficients is using. Due to this, significant non-oscillating property of scheme is obtained, which increases its order of accuracy.

The solution of the algebraic equation for the temperature field is performed with using an iterative method of Newton-Raphson with second order of convergence

$$f(T) = E_t - \frac{\rho}{\gamma_\infty M_\infty^2 W}\left(\tilde{H}(T) - RT\right) - \frac{1}{2}\rho\left(u^2 + w^2\right) = 0,$$

where $\tilde{H}$ is molar enthalpy of gaseous mixture.

RESULTS AND ITS ANALYSIS

Computer code is validated by the simulation of incident shock wave turbulent boundary layer interaction. Namely, supersonic flow along the thin plate is considered with the shock generator at the top wall. The parameters of problem are taken from experiment [9], where Mach number of the flow is $M_\infty = 5$, Reynolds number is $Re = 40 \cdot 10^6$, temperature of the wall is $T_w = 300K$. The angle of shock generator is equal to $\alpha = 14^o$, which corresponds to the separated flow of boundary layer. The comparison of experimental and numerical results shows good agreement.

Results of the numerical simulations of considering problem are presented below.

Figure 1 (1a - $n_1 = 5$, 1b - $n_2 = 15$, 1c - $n_3 = 25$) shows the picture of shock-wave structures in the regions of the jet injection which are analogous to structures that have been obtained by symmetric upper boundary conditions [7]. Namely, due to the deceleration of incoming flow, the pressure increases, and a bow shock wave 1 is formed. Oblique shock wave 2 is emanated from the bow shock wave, which moves to the entrance boundary during the growth of the pressure ratio. In this separation zone the additional supersonic flow region exists behind the oblique shock, which promotes the formation of the closing shock 3 parallel to the jet axis.

The bow shock wave 1 (the incident shock wave) reaches the upper boundary layer of the planar channel and interacts with it. The propagation of the pressure gradient in the subsonic regions induces compression waves, which converge into the reflected shock wave 4. This shock wave intersects with the incident (bow) shock and wave 4 is transmitted as shock 5, while bow shock continue its traveling up.

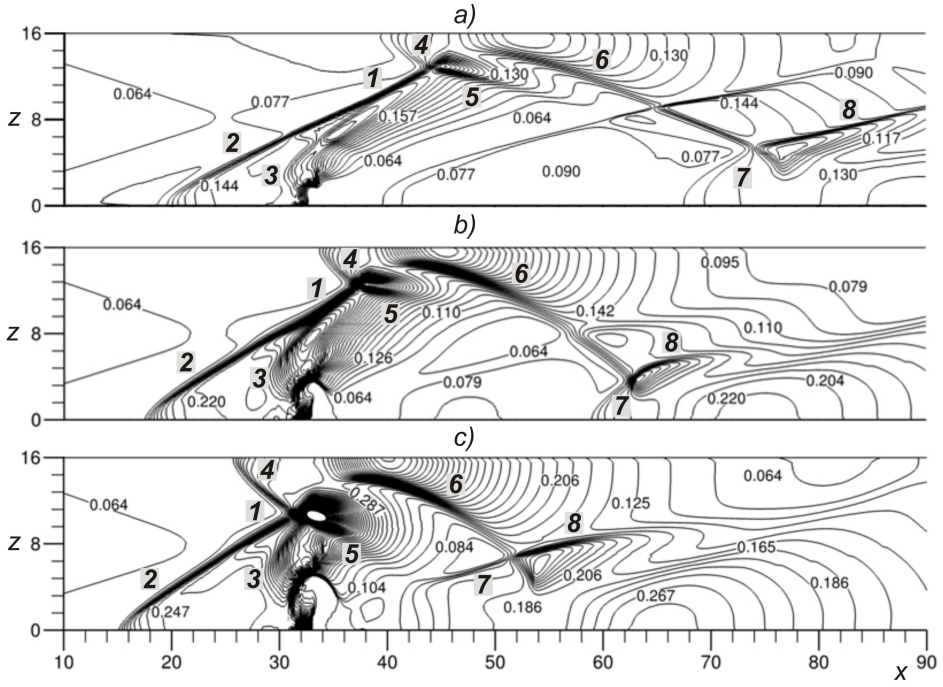

FIGURE 1. Distribution of the isobars for pressure ratio $n_1 = 5$ (a), $n_2 = 15$ (b) and $n_3 = 25$ (c)

The bow shock penetrates into the shear layer and is reflected as an expansion fan in the sonic line. Here separation bubble appears, which deflects towards the wall due to the expansion fan. Finally, the reattachment shock 6 appears due to the reattachment of this separation zone downstream.

From Figure 1 (a,b,c) a new system of shock-wave structures is seen due to the shock wave boundary layer interaction at the bottom wall. Namely, the compression wave 6 reaches bottom boundary layer in the region behind jet and here the separation bubble appears due to pressure gradients, which is large enough. Then reflected shock wave 7 is formed, which after intersections with wave 6 traveling as wave 8.

It is seen (Figure 1) that described above shock-wave structures are observed for all three cases.

The picture of vector fields of the velocities - Figure 2 for different pressure ratio (2a - $n_1 = 5$, 2b - $n_2 = 15$, 2c - $n_3 = 25$) demonstrates that the recirculation zones ahead and behind of jet are increased with the growth of the pressure ratio. Numerical experiment shows that the vortex system are similar to the vortices, which have been presented in [7]. Ahead of the jet in the zone adjacent to the wall, two vortices are formed as a result of primary and secondary separations of the flow. These vortices rotate in the opposite directions. The first vortex, located at the same distance upstream of the jet, is rotated clockwise, the second vortex, located closer to the jet, moves anticlockwise. The vortex behind the jet is formed due to the presence of low-pressure zones in this region.

It is seen (Figure 2) that the vortex structure at upper boundary was formed due to shock wave boundary layer interaction. The size of the separation bubble is growing and moving upstream with the increase of the pressure ratio (Figure 2 (a,b,c)).

Additional separation is obtained during the shock wave boundary layer interaction on the bottom wall behind the jet (Figure 2).

It can be seen from Figure 2 (a,b,c) the intensity of shock wave 6 is enough to cause separation bubble at lower boundary layer behind the jet, and how it follows from figures, with the growth of the pressure ratio, recirculation zone moves to the entrance with increasing in size.

Figure 3 shows numerical experiment the effect of the pressure ratio on the jet penetration. The curve indicates the penetration for 0.1% hydrogen concentration for pressure ratio in the range $5 \leq n \leq 35$. From figure follows that the height of the jet penetration also increases with the increase of the pressure ratio.

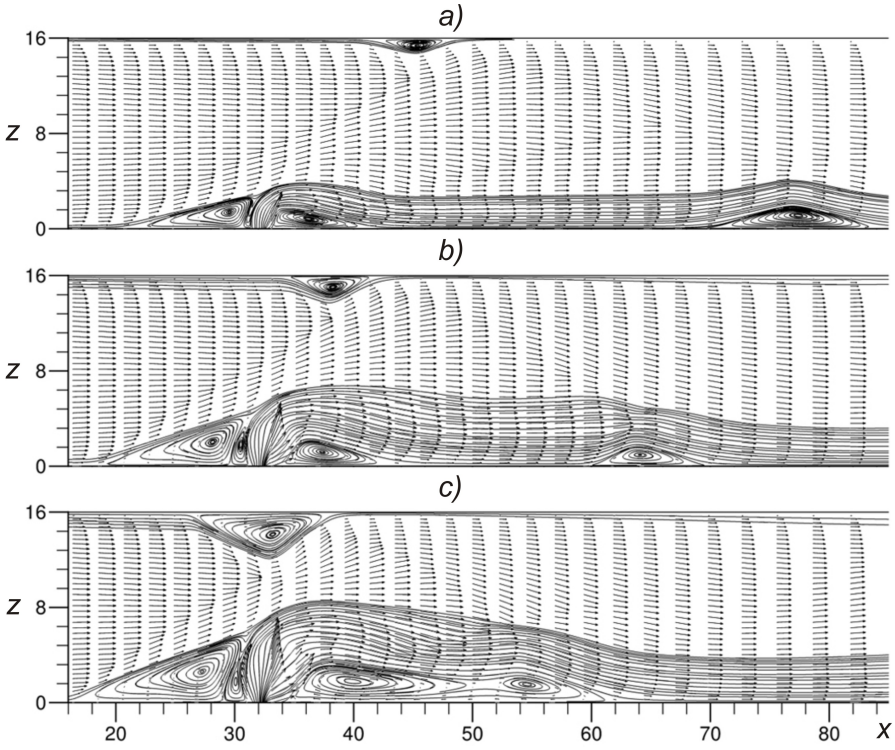

FIGURE 2. Vector fields of the velocities for pressure ratio $n_1 = 5$ (a), $n_2 = 15$ (b) and $n_3 = 25$ (c)

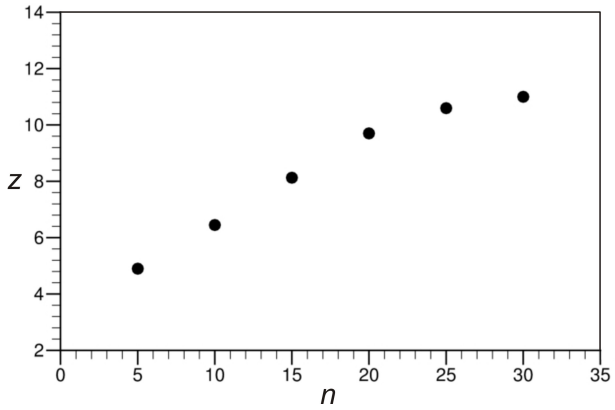

FIGURE 3. Dependence of the pressure ratio and the jet penetration

REFERENCES

1. A. I. Glagolev, and A. I. Zubkov, *Izv. Akad. Nauk SSSR, Mekh. Zhidk. Gaza* **2**, 99–102 (1968).
2. V. S. Avduevskii, and K. I. Medvedev, *Izv. Akad. Nauk SSSR, Mekh. Zhidk. Gaza* **5**, 193–197 (1970).
3. V. Viti, and S. Wallis, *AIAA Journal* **42**, 1358–1368 (2004).
4. S. Tomioka, and L. S. Jacobsen, *Journal of Propulsion and Power* **19**, 104–114 (2003).
5. P. A. Polivanov, and A. A. Sidorenko, *Technical Physics Letters* **19**, 29–37 (2015).
6. V. Pasquariello, and M. Grilli, *International Journal of Heat and Fluid Flow* **49**, 116–127 (2014).
7. A. O. Beketaeva, and A. Z. Naimanova, *Journal of Applied Mechanics and Technical Physics* **45**, 367–374 (2004).
8. X. Liu, and S. Osher, *Journal of Computational Physics* **115**, 200–212 (1994).
9. N. N. Fedorova, and I. A. Fedorchenko, *Journal of Applied Mechanics and Technical Physics* **45**, 358–366 (2004).